Aerodynamic Optimization of Rocket Control Surfaces Using Cartesian Methods and CAD Geometry

Andrea Nelson,* Michael J. Aftosmis,† Marian Nemec,‡
and Thomas H. Pulliam§

NASA Ames Research Center
MS T27B-1, Moffett Field, CA 94035

Abstract submitted to the 23rd AIAA Applied Aerodynamics Conference
Jun. 6–9, 2005, Toronto, Ontario

I. Introduction

Aerodyanamic design is an iterative process involving geometry manipulation and complex computational analysis subject to physical constraints and aerodynamic objectives. A design cycle consists of first establishing the performance of a baseline design, which is usually created with low-fidelity engineering tools, and then progressively optimizing the design to maximize its performance. Optimization techniques have evolved from relying exclusively on designer intuition and insight in traditional "trial and error" methods, to sophisticated local and global search methods.

Recent attempts at automating the search through a large design space with formal optimization methods include both database driven and direct evaluation schemes. Databases are being used in conjunction with surrogate and neural network models as a basis on which to run optimization algorithms. Optimization algorithms are also being driven by the direct evaluation of objectives and constraints using high-fidelity simulations.

Surrogate methods use data points obtained from simulations,[1,2] and possibly gradients evaluated at the data points,[3] to create mathematical approximations of a database. Neural network models[4,5] are work in a similar fashion, using a number of high-fidelity database calculations as training iterations to create a database model.

Optimal designs are obtained by coupling an optimization algorithm to the database model. Evaluation of the current best design then gives either a new local optima and/or increases the fidelity of the approximation model for the next iteration. Surrogate methods have also been developed that iterate on the selection of data points to decrease the uncertainty of the approximation model prior to searching for an optimal design.[6] The database approximation models for each of these cases, however, become computationally expensive with increase in dimensionality. Thus the method of using optimization algorithms to search a database model becomes problematic as the number of design variables is increased.

In contrast to the above methods that rely on databases, direct performance evaluations can be used to form an automatic iteration loop that is connnected to the manipulation of the geometry via an optimization

*PhD student, Stanford University, anajn@stanford.edu
†Research Scientist, Senior Member AIAA
‡NRC Research Associate, Member AIAA
§Associate Fellow AIAA, tpulliam@mail.arc.nasa.gov

algorithm.[7] With this method, optimization algorthims query the high performance simulation directly, becoming most effective when combined with a fast evaluation of design sensitivities, inparticular adjoint methods.[8]

In this paper we employ recently developed automatic database creation and geometry manipulation tools to aid in the evaluation of optimization techniques. Prior to beginning the optimization work, an aerodynamic performance database can be automatically produced[9] to fully understand the performance characteristics of the baseline design. After optimization, a similar database is created to evaluate the final design.

Geometry manipulation is used both with database generation and with direct evaluation optimization methods. The automatic database generation along with the geometry manipulation analyzes multiple configurations using a single representative point in the performance envelope. The resulting database is a basis for gradient based and evolutionary algorithms in a database searching optimization approach. In addition to the geometry manipulation coupled with the high-fidelity solver, we also employ an adjoint method as a driect evaluation optimization algorithm.[7,10]

The evaluation of the optimization techniques is demonstrated on the design of a suborbital rocket. Results presented in this abstract include the baseline performance database, direct performance evaluations and "trial and error" design iterations. Discussions of these results focus on the influence of the design variables on the objective and constraints, and the effectiveness of the iterations on convergence toward a viable control surface configuration.

II. Problem Formulation

The design of a suborbital rocket in ascent configuration is presented. The baseline design of the rocket was created subject to a real-world constraint on the maximum diameter of the vehicle to assure that the rocket fits under standard highway overpasses during transport via truck and trailer. The preliminary design of the vehicle was analyzed with the steady-state Cartesian solver of Aftosmis *et al.*[11] through a parameter study over a range of both Mach numbers and angle-of-attack. This baseline analysis revealed a pitch instability for the ascent configuration. The redesign of the vehicle is undertaken to produce a negative, or stable, Cm_α. The geometry and location of the six control surfaces, or fins, are varied in order to move the center of pressure of the vehicle to a specified position aft of the center of gravity.

Using a recently developed approach that allows direct access to the geometry via the native CAD model, it is possible to modify the design variables and evaluate geometric constraints as parameters of the CAD master-model feature tree. This approach is *vendor neutral*, i.e. independent of a specific CAD system, and is based on the Computational Analysis and PRogramming Interface (CAPRI).[12,13,14] Coupling this approach with the fast and robust Cartesian mesh generation,[15,16] the interface between geometry and solver can essentially be fully automatic. In addition, the use of this approach along with optimization algorithms allows for a design iteration process that is more efficient than can be accomplished by hand.

The aerodynamic optimization problem consists of determining values of design variables X, such that the objective function $\mathcal{J}$ is minimized

$$\min_X \ \mathcal{J}(X, Q) \tag{1}$$

subject to constraint equations C_j:

$$C_j(X, Q) \leq 0 \qquad j = 1, \ldots, N_\mathrm{c} \tag{2}$$

where the vector Q denotes the conservative flowfield variables and N_c denotes the number of constraint equations. The flowfield variables are forced to satisfy the governing flowfield equations, $\mathcal{F}$, within a feasible region of the design space Ω:

$$\mathcal{F}(X, Q) = 0 \qquad \forall \ X \in \Omega \tag{3}$$

which implicitly defines $Q = f(X)$. The governing flow equations are the three-dimensional Euler equations of a perfect gas, where the vector $Q = [\rho, \rho u, \rho v, \rho w, \rho E]^T$.

For the problem under consideration here, the objective function is given by

$$\mathcal{J} = \begin{cases} \omega_{\mathrm{M}} \left(1 - \frac{C_{\mathrm{M}}}{C_{\mathrm{M}}^{*}}\right)^{2} + \omega_{\mathrm{D}} \left(1 - \frac{\mathrm{D}}{\mathrm{D}^{*}}\right)^{2} & \text{if } \mathrm{D} > \mathrm{D}^{*} \\ \omega_{\mathrm{M}} \left(1 - \frac{C_{\mathrm{M}}}{C_{\mathrm{M}}^{*}}\right)^{2} & \text{otherwise} \end{cases} \tag{4}$$

where D^{*} and C_{M}^{*} represent the target diameter and moment coefficient, respectively. The weights ω_{D} and ω_{M} are user specified constants. The design variables chosen for the parameterization of the fins, shown in Fig. 1(a), are axial position of the leading edge, X_{le}, maximum thickness, t_{max}, location of maximum thickness, $X_{\mathrm{t_{max}}}$, and total length of the fin, L.

III. Numerical Methods

The details of the numerical methods will be provided in the complete paper. Only a brief summary is given here.

The solver used for the analysis of these cases is the Cartesian inviscid-flow analysis package, Cart3D, of Aftosmis *et al.*[16,11] The flow is solved to a steady state, while using specified exhaust boundary conditions[17] to simulate the engine exhaust. The preliminary configuration was run to create a database of aerodynamic coefficients over a sweep of Mach numbers and angles of attack.

The primary techniques to be employed in the automated design optimization are the genetic algorithm of Holst and Pulliam,[18] and an unconstrained BFGS quasi-Newton algorithm coupled with a backtracking line search.[10]

IV. Results and Discussion

The rocket in ascent configuration as shown in Fig. 1 consists of a central body, six engines at the base of the rocket, and six fins located just forward of the base. The fins in their original configuration have a maximum radial thickness located near the fore end of each fin, where the diameter of the vehicle is less, in order to decrease the maximum diameter of the vehicle. The result of this design is a forward location of the center of pressure on each fin which leads to a positive pitching moment of the vehicle.

The initial "trial and error" method used here to pursue a more optimal design iterates on the fin geometry and location. The surface discretization of each fin in the radial or axial direction is rescaled and the axial location of the leading edge is modified. Following each iteration of geometry manipulation, the volume mesh is recomputed and analyzed with the flow solver.

For this extended abstract the surface geometry is modified using an in-house grid modification toolkit, OVERGRID.[19,20] The variables available for modifications are scaling factors in the x, y, and z directions. In order to use these as design variables, a singular fin aligned with the y-axis is used for modifications and is subsequently rotated around the vehicle to replace the other fins. The resulting design variables used in the manual iteration procedure are radial scaling (or scaling in the y-axis direction) and axial scaling (in the x-axis direction). In addition to these variables, the axial position of the fin was used to keep it as far aft on the rocket as possible while maintaining contact with the surface of the vehicle.

The current results obtained via baseline database and manual design iteration are presented here. Results of the redesign via optimization algorithms will be presented in the complete paper.

The initial configuration was used to create a baseline database of aerodynamic coefficients to assess the stability of the vehicle using the flow solver over a range of freestream Mach numbers, M_{∞}, and angles of attack, α. Figure 2 shows C_{L}, C_{M} and C_{D}. Reviewing the carpet plot of C_{M} reveals that the vehicle is unstable in pitch such that increasing α produces an increasing pitching moment. Using the desired location of center of gravity, post processing indicates this unstable positive increase in pitching moment with increase in angle of attack, or a positive Cm_{α}, for all subsonic and transonic Mach numbers included in the analysis.

The results of the baseline database show the greatest positive Cm_{α} occurring for subsonic Mach numbers.

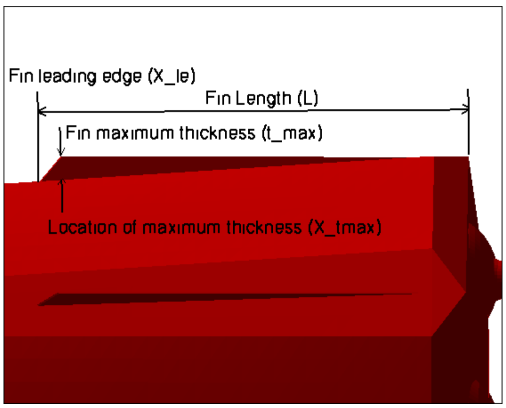

(a) Fin parameterization

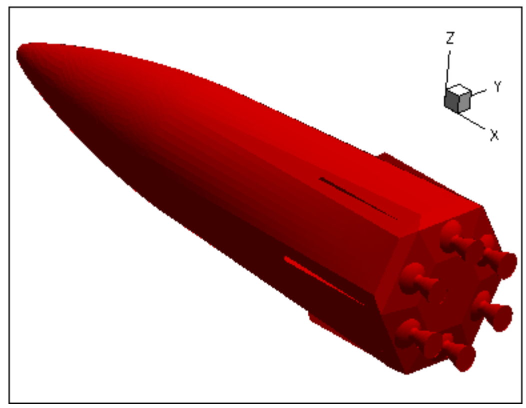

(b) Isometric view of baseline design

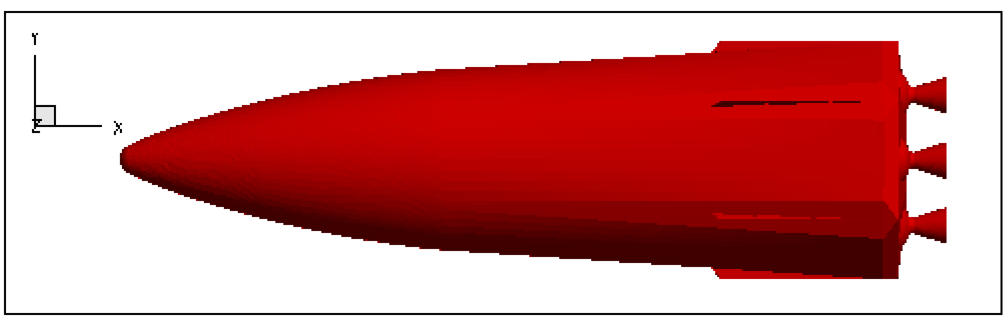

(c) Top view of baseline design

Figure 1. Suborbital vehicle baseline design, ascent configuration

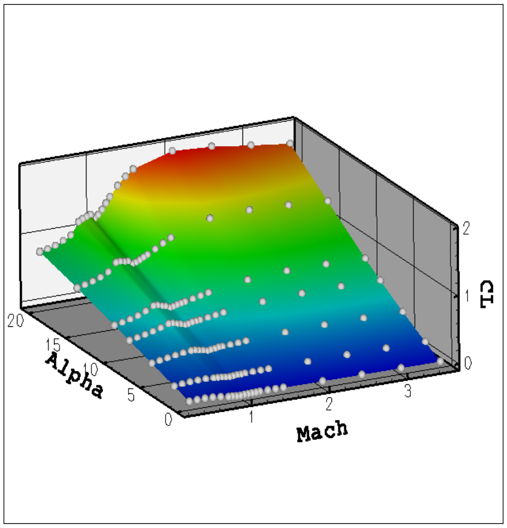

(a) Carpet plot of C_L vs. M_∞ and α

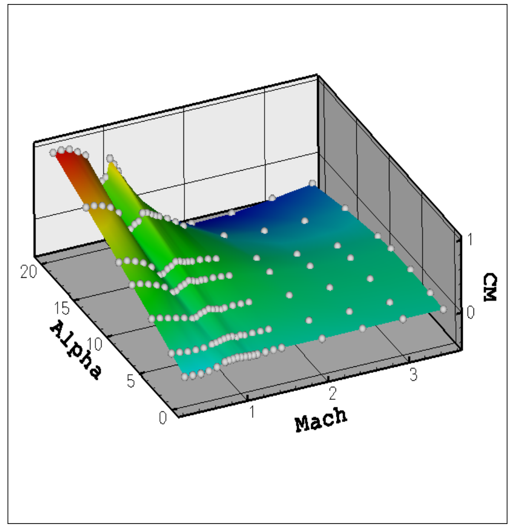

(b) Carpet plot of C_M vs. M_∞ and α

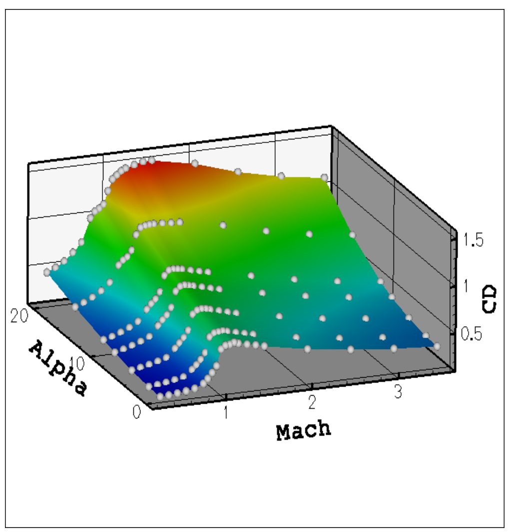

(c) Carpet plot of C_D vs. M_∞ and α

Figure 2. Results of baseline database analysis

Based on this observation, all manual design iterations were evaluated at an M_∞ of 0.6 and α of 20°. For the original design at an M_∞ of 0.6 and α of 20°, the resulting C_M is 0.874, evaluated about an x_{cg} of 325 (inches) as measured from the nose of the vehicle. The initial design iterations using radial scaling were analyzed for scaling factors of 2.5 and 5.0, resulting in C_M values of 0.454 and -0.0236 respectively. The results indicate the radial scaling factor of 5.0 produces a fin with negative C_M, but it also increases the maximum diameter by 33%. The subsequent iteration was analyzed using a radial scaling factor of 5.0 and an axial scaling factor of 1.77 to decrease the vehicle maximum diameter. The resulting C_M was 0.206, while the maximum vehicle diameter increase was reduced to 28%. The pressure distribution of the configuration using a radial scaling factor of 5.0 is shown in Fig. 3. The pressure distribution of the configuration with a radial scaling factor of 5.0 and axial scaling factor 1.77 is shown in Fig. 4.

The effect of scaling the fins radially is to increase the effective area while having little effect on the location of the center of pressure for each fin. Consequently, the higher area will increase the lift of the fins at an angle of attack, while maintaining relatively the same moment arm around the center of gravity of the vehicle. The first set of design iterations focus on only radial scaling to determine the amount of scaling necessary to achieve a negative Cm_α at an α of 20°.

Scaling in the axial direction creates more fin area while decreasing the overall diameter of the vehicle. However, this method of scaling also brings the center of pressure of the fins forward, causing the lift created by the fins to be less effective in creating a pitch-down moment at positive angles of attack. The second set of design iterations focus on combining both radial and axial scaling in order to achieve the negative Cm_α, while not exceeding the maximum diameter as specified.

V. Summary

Results of a preliminary analysis database on the suborbital launch vehicle indicate an unstable positive Cm_α for subsonic and transonic conditions. Design iterations performed by manually modifying the surface discretization of the launch vehicle control surfaces through radial scaling demonstrate an improvement in the objective but violate the constraint on vehicle diameter. Iterations involving axial scaling diminish the effect on vehicle diameter, but do not succeed in obtaining the objective C_M.

The full paper will extend the results by performing a complete optimization analysis coupled directly with the CAD model. This fully-coupled analysis will allow more possible control surface configurations. In addition both gradient based and evolutionary algorithm optimization methods will be applied to the design problem to produce a configuration that best satisfies the objective of increased static stability while minimizing the vehicle diameter.

References

[1]Booker, A. J., Jr., J. E. D., Frank, P. D., Serafini, D. B., Torczon, V., and Trosset, M. W., "A Rigorous Framework for Optimization of Expensive Functions by Surrogates," Technical Report CRPC–TR98739–S, Center for Research on Parallel Computation, Houston, TX, Feb. 1998.

[2]Rodriguez, D. L., "Response Surface Based Optimization With a Cartesian CFD Method," AIAA Paper 2003–0465, Jan. 2003.

[3]Chung, H. and Alonso, J. J., "Design of a Low-Boom Supersonic Business Jet Using Cokriging Approximation Models," AIAA Paper 2002–5598, Atlanta, GA, 2002.

[4]Greenman, R. and Roth, K. R., "Minimizing Computational Data Requirements for Multi-Element Airfoils Using Neural Networks," *Journal of Aircraft*, Vol. 36, No. 5, 1999, pp. 777–784.

[5]Greenman, R., Stepniewski, S. W., Jorgensen, C. C., and Roth, K. R., "Designing Compact Feedforward Neural Models with Small Training Data Sets," *Journal of Aircraft*, Vol. 39, No. 3, 2002, pp. 452–459.

[6]Gramacy, R. B., Lee, H. K. H., and Macready, W. G., "Parameter Space Exploration with Gaussian Process Tree," *Proceedings of the International Conference on Machine Learning*, 2004, pp. 353–360.

[7]Nemec, M., Aftosmis, M. J., and Pulliam, T. H., "CAD-Based Aerodynamic Design of Complex Configurations Using a Cartesian Method," AIAA Paper 2004–0113, Reno, NV, Jan. 2004.

[8]Leoviriyakit, K., Kim, S., and Jameson, A., "Aero-Structural Wing Planform Optimization Using the Navier-Stokes Equations," AIAA/ISSMO Paper 2004–4479, Albany, NY, Aug. 2004.

[9]Murman, S. M., Aftosmis, M. J., and Nemec, M., "Automated Parameter Studies Using a Cartesian Method," AIAA Paper 2004–5076, Providence, RI, Aug. 2004.

[10]Nemec, M. and Zingg, D. W., "Newton–Krylov Algorithm for Aerodynamic Design Using the Navier–Stokes Equations," *AIAA Journal*, Vol. 40, No. 6, 2002, pp. 1146–1154.

[11]Aftosmis, M. J., Berger, M. J., and Adomavicius, G., "A Parallel Multilevel Method for Adaptively Refined Cartesian Grids with Embedded Boundaries," AIAA Paper 2000–0808, Reno, NV, Jan. 2000.

[12]Haimes, R. and Follen, G., "Computational Analysis PRogramming Interface," *Proceedings of the 6th International Conference on Numerical Grid Generation in Computational Field Simulations*, edited by Cross, Eiseman, Hauser, Soni, and Thompson, University of Greenwich, 1998.

[13]Aftosmis, M. J., Delanaye, M., and Haimes, R., "Automatic Generation of CFD-Ready Surface Triangulations from CAD Geometry," AIAA Paper 99–0776, Reno, NV, Jan. 1999.

[14]Haimes, R. and Aftosmis, M. J., "On Generating High Quality "Water-tight" Triangulations Directly from CAD," Tech. rep., Meeting of the International Society for Grid Generation, (ISGG), Honolulu, HI, June 2002.

[15]Aftosmis, M. J., "Solution Adaptive Cartesian Grid Methods for Aerodynamic Flows with Complex Geometries," Lecture notes, von Karman Institute for Fluid Dynamics, Series: 1997-02, Brussels, Belgium, March 1997.

[16]Aftosmis, M. J., Berger, M. J., and Melton, J. E., "Robust and Efficient Cartesian Mesh Generation for Component-Based Geometry," *AIAA Journal*, Vol. 36, No. 6, 1998, pp. 952–960.

[17]Pandya, S. A., Murman, S. M., and Aftosmis, M. J., "Validation of Inlet and Exit Boundary Conditions for a Cartesian Method," AIAA Paper 2004–4837, Aug. 2004.

[18]Holst, T. L. and Pulliam, T. H., "Aerodynamic Shape Optimization Using a Real-Number-Encoded Genetic Algorithm," AIAA Paper 2001–2473, Anaheim, CA, June 2001.

[19]Chan, W. M., "Innovative Software Streamlines Overset Grid Generation," *NAS News*, Vol. 3, No. 3, 2004, pp. 353–360.

[20]Chan, W. M., "OVERGRID - A Unified Overset Grid Generation Graphical Interface," *Electronic Journal of Grid Generation, Special Chimera Issue*, 1999.

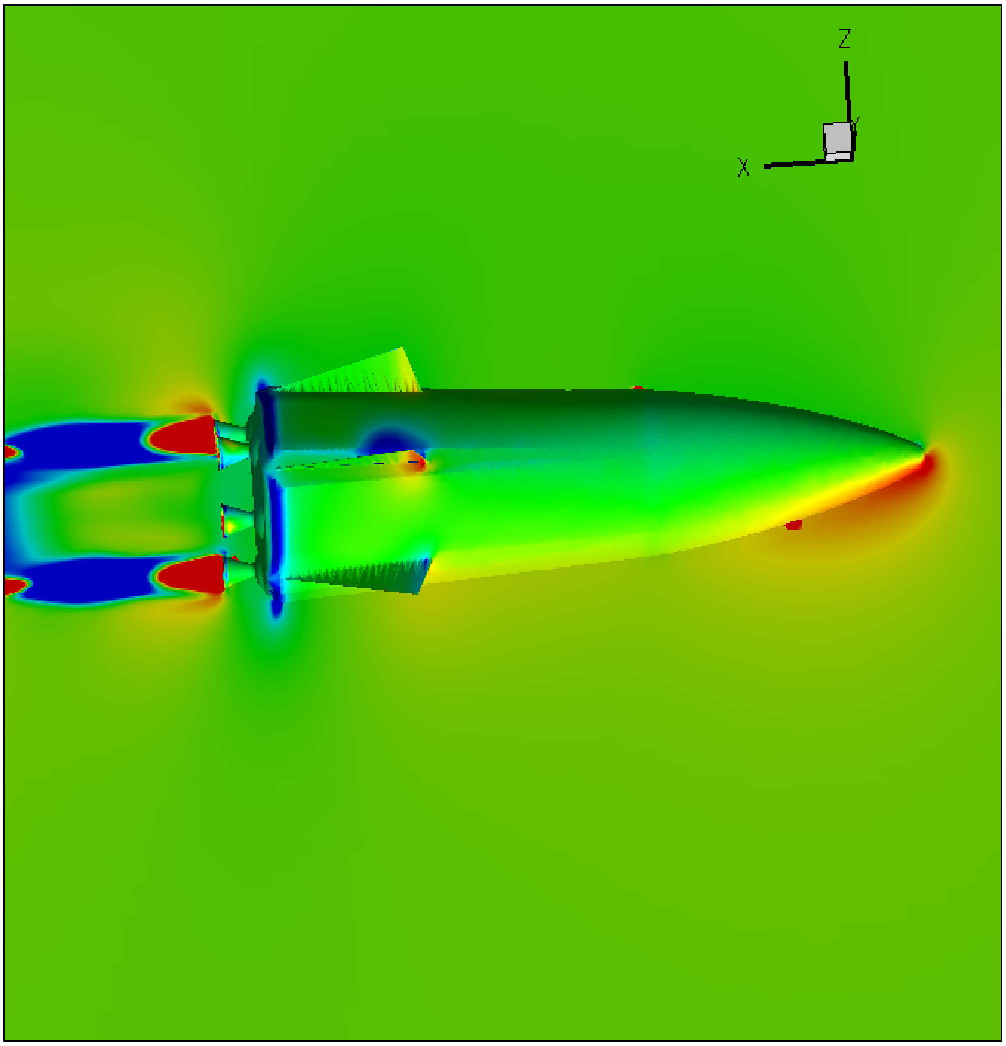

Figure 3. Surface pressure distribution for initial fin configuration using radial scaling factor, $M_\infty = 0.6$, $\alpha = 20°$, $radial scaling factor = 5.5$

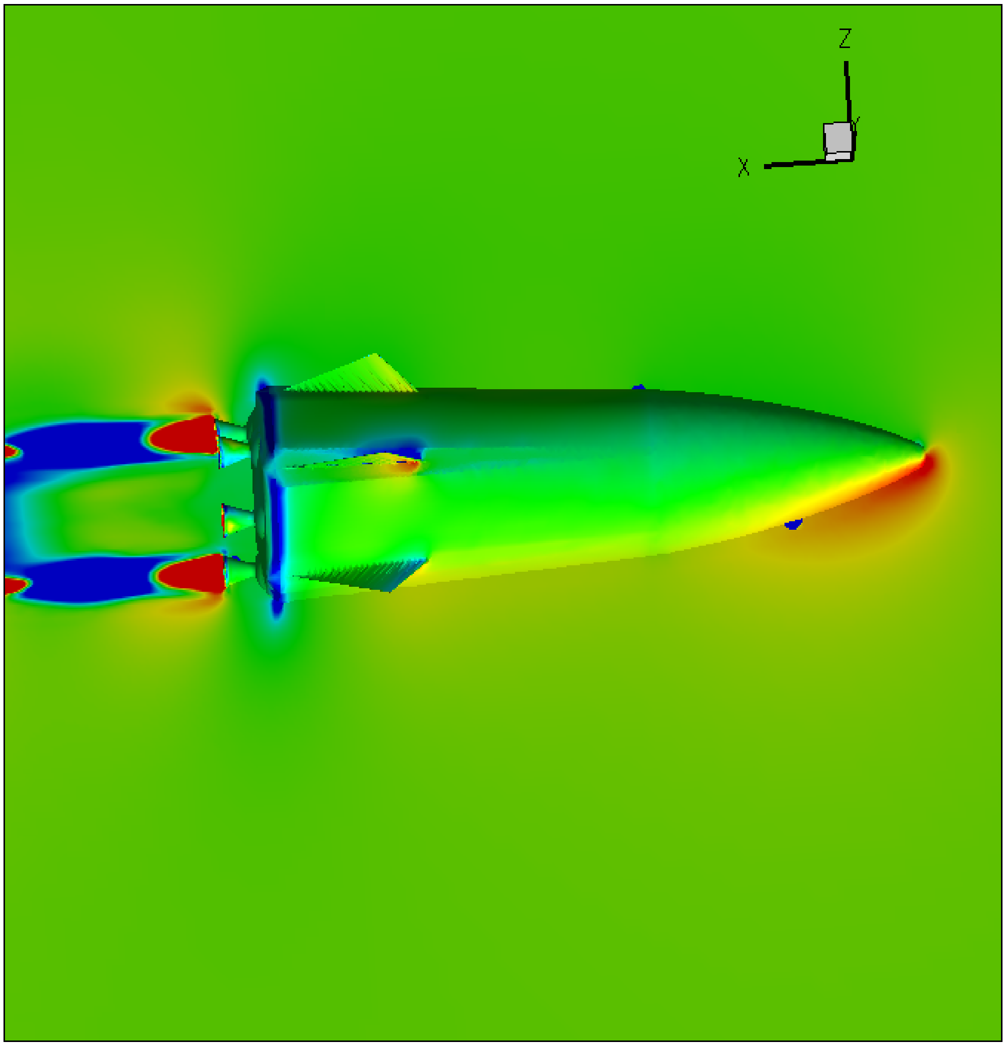

Figure 4. Surface pressure distribution for initial fin configuration using axial scaling factor and axial location, $M_\infty = 0.6$, $\alpha = 20°$, $radialscalingfactor = 5.5$, $axialscalingfactor = 1.77$